JOURNAL OF GEOPHYSICAL RESEARCH, VOL. 93, NO. D2, PAGES 1361–1375, FEBRUARY 20, 1988

Structure and Growth of the Mixing Layer Over the Amazonian Rain Forest

CHARLES L. MARTIN,[1] DAVID FITZJARRALD,[2] MICHAEL GARSTANG,[3]
AMAURI P. OLIVEIRA,[4] STEVE GRECO,[3] AND EDWARD BROWELL[5]

Measurements carried out over the rain forest of central Amazonia during the NASA Amazon Boundary Layer Experiment (ABLE 2A) are used to examine the structure and growth of the atmospheric mixed layer. Fluxes of sensible and latent heat were measured at the top of the canopy, and measurements of temperature, moisture, and horizontal wind were made in and above the mixed layer by means of a tethered balloon, rawinsonde, and aircraft. The mixing layer grows rapidly at 5–8 cm s^{-1} soon after sunrise to a mean maximum height of 1200 m by 1300 local standard time (LST). Mixed layer heights above 1000 m between 1000 and 1600 LST are common during undisturbed conditions. Fossil mixed layers, well mixed but no longer mixing, were found to 2000 m and at all times of the day and night. Airborne lidar measurements provided an estimate of the depth of the mixed layer over large distances. No horizontal inhomogeneities in the mixed layer structure or depth were found over large distances, suggesting that point measurements under undisturbed conditions can be used to obtain estimates of mixed layer structure and fluxes over large areas of the Amazon basin. Budget calculations using the averaged mixed layer depths and surface fluxes are made, which provide estimates of the entrainment flux of moisture across the mixed layer top of the order of 600 W m^{-2}. The simple jump model, when initialized with an early-morning sounding and forced with observed buoyancy fluxes, is compared with the budget calculation and observations. The entrainment flux calculations agree favorably. Flux divergence in the mixed layer leads to significant drying, which is observed at the top of the canopy.

1. INTRODUCTION

The Amazon rain forest has been recognized as a major source region of atmospheric trace gases and aerosols [*National Academy of Sciences*, 1984; *Fishman et al.*, 1986; *Logan and Kirchhoff*, 1986]. Species that are produced or consumed in the forest are transported between forest and the troposphere through the atmospheric boundary layer. During the day there is a dry convective boundary layer coupling the canopy to the deeper atmosphere through turbulent mixing. In this paper we refer to this region as the mixed layer. The behavior of this layer is critical in determining the transport of species to the deeper atmosphere and their concentrations there. Very little data are available which document the structure and processes of the atmospheric mixed layer over such a vast and inaccessible region as the Amazon basin. The few rawinsonde stations which do carry out one or two operational soundings per day in the basin provide infrequent sampling, and the vertical resolution of the operational rawinsonde is not good enough to describe the structure of the mixed layer.

A major purpose of the NASA Amazon Boundary Layer Experiment (ABLE 2A) was to obtain a quantitative description of the mixed layer at a single forest location and to obtain estimates of the spatial homogeneity or inhomogeneity of the mixed layer away from this location by means of a research aircraft. The field program was designed to obtain high time and space resolution measurements over a period of about 3 weeks during the mainly undisturbed weather of the dry season in July and August 1985.

In this paper we will present a description of the mixed layer characteristics above the Amazonian rain forest during undisturbed conditions. This information has not previously been available and will be of relevance to other atmospheric studies of the Amazon basin. Following this description, we present estimates of the entrainment flux of moisture at the top of the mixed layer, this being derived from the measured surface fluxes and the mixed layer characteristics. It is hoped that an analogy between water vapor and other chemical species can be made and directed at gaining an understanding of how a large suite of important chemical species and aerosols [*Harriss et al.*, this issue] generated in the soils, in the forest canopy, and above the canopy are communicated between the canopy and the deeper atmosphere. A simple mixed layer model is applied to show how fluxes of species might be estimated using only quantities measured at the surface and prescribing an initial condition and boundary condition for the mixed layer. Finally, mixing line analysis is used to discuss the growth of an actively mixing layer into a previous, or "fossil," mixed layer.

2. FIELD MEASUREMENTS

ABLE 2A, described by *Harriss et al.* [this issue], was based on Manaus (2°S, 60°W) in central Amazonia (Figure 1). Measurements were made from July 15, to August 7, 1985, under weather conditions characteristic of the early dry season. Thus while showers (25–55 mm of rain per day at an individual station) occurred on the first few days of the experiment in the Manaus region, dry conditions characteristic of the subtropical anticyclone became increasingly common from July 17 onward. Convective activity in the form of large cloud complexes continued to occur to the west of Manaus throughout the experiment. Manaus often lay just inside the fair-weather region, on the boundary between the suppressed con-

[1] Simpson Weather Associates, Incorporated, Charlottesville, Virginia.
[2] Atmospheric Sciences Research Center, State University of New York, Albany.
[3] Department of Environmental Sciences, University of Virginia, Charlottesville.
[4] Departamento de Meteorologia, Instituto Astrônomico e Geofisico, Universidade de São Paulo, São Paulo, Brasil.
[5] NASA Langley Research Center, Hampton, Virginia.

Paper number 7D0694.
0148-0227/88/007D-0694$05.00

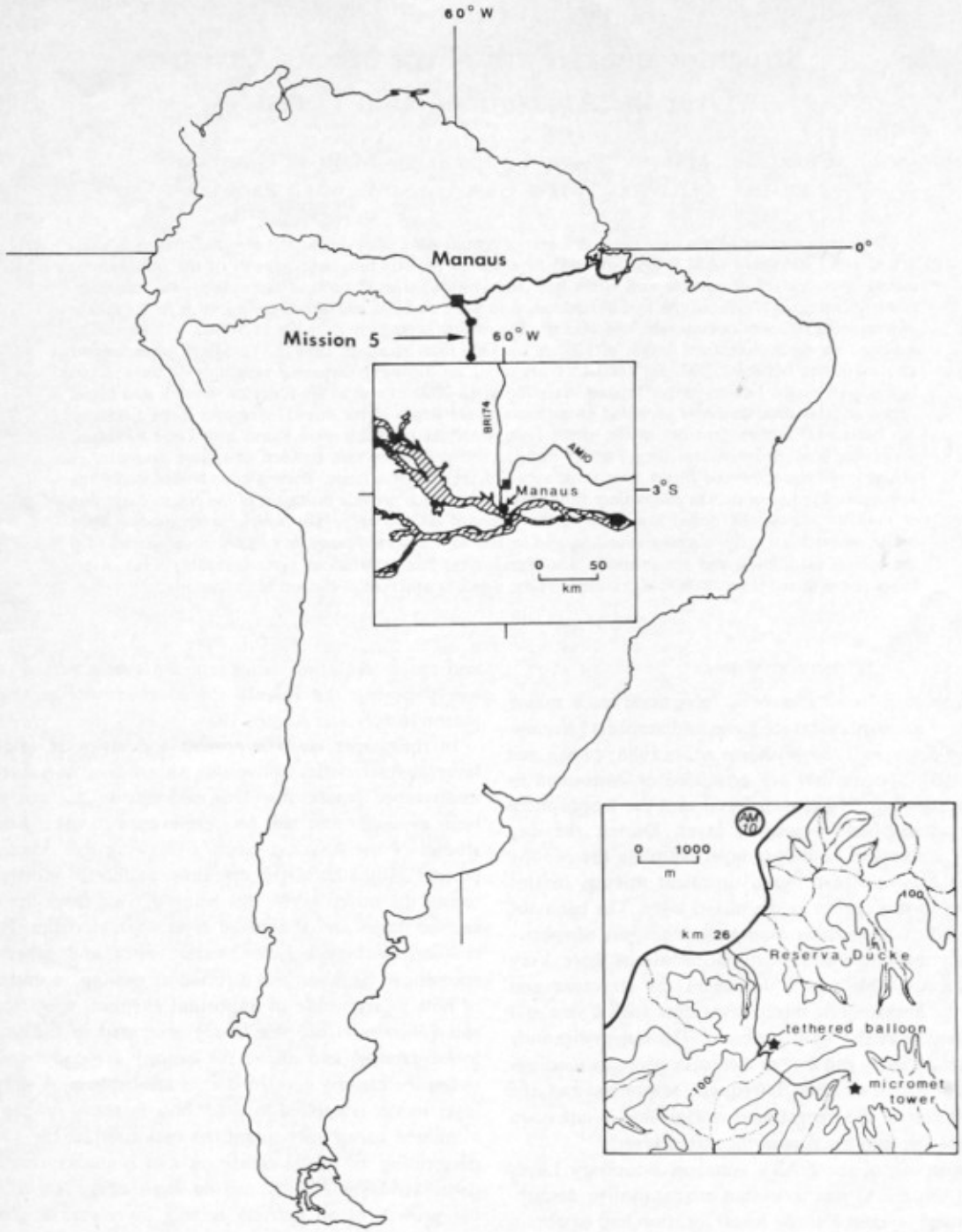

Fig. 1. Location of the ABLE 2A experiment. Ground-based measurements were made at Reserva Ducke, shown in inset box. The 100-m ground elevation contour and stream courses are given for the area southeast of highway AM10. Flight track for mission 5 is shown south of Manaus.

ditions of the anticyclone and active convection to the west of Manaus.

Ground-based measurements (Table 1) were made from the Ducke Forest Reserve, located about 20 km northeast of Manaus (Figure 1). Ground elevations in the reserve average 90 m above mean sea level (MSL), while the height of the forest canopy is about 35 m. Thus the top of the canopy is approximately 125 m above MSL. In this paper all elevations are referenced to sea level unless otherwise noted.

Heat, moisture, and momentum fluxes were calculated at two levels, 5 and 10 m above the top of the forest canopy, using fast-response measurements from instrumentation mounted on top of a micrometeorological tower. These measurements are described by *Fitzjarrald et al.* [this issue]. The eddy flux measurements were edited to remove periods of bad data, which were known to occur when sensors failed [*Fitzjarrald et al.*, this issue]. These problems were not common, and the data return for the eddy flux measurements

TABLE 1. Summary of the Data Set

Date	Tethered Balloon Night Operations	Tethered Balloon Profiles	Ducke Rawinsonde Soundings	Aircraft Flight	Tower Flux Measurements	Tower Weather Station
July 15		13	3		N	Y
July 16		18	4		N	Y
July 17		13	4		N	Y
July 18		14	4	day	N	Y
July 19		21	4	day	N	Y
July 20		7	4		N	Y
July 21		15	4	day	N	Y
July 22		22	4		Y	Y
July 23		13	4	day	Y	Y
July 24		15	3	day	Y	Y
July 25	Y	20	6		Y	Y
July 26	Y	24	8	night	Y	Y
July 27		21	6	night	Y	Y
July 28					Y	Y
July 29		12	3		Y	Y
July 30	Y	9	2	day	Y	Y
July 31	Y	49	9	day	Y	Y
Aug. 1	Y	20	8		Y	Y
Aug. 2	Y	44	8	day	Y	Y
Aug. 3		30	5	day	Y	Y
Aug. 4		24	4		Y	Y
Aug. 5		27	2	day	Y	Y

Y indicates observations; N, no observations.

was approximately 77%. The upper and lower levels of the eddy flux data were observed to be very similar [*Fitzjarrald et al.*, this issue]. In the following calculations, data was used from the lower level at 39 m, approximately 5 m above the canopy.

An automatic weather station on the same tower provided mean values of temperature, moisture, and horizontal wind velocity [*Shuttleworth et al.*, 1984].

Temperature, humidity, pressure, and horizontal wind speed and direction were measured by a tethered balloon-borne sonde profiling at the rate of 1 m s^{-1} between 10 and 1100 m above the ground. Measurements were made every 10 s, providing a vertical resolution of 10 m. Each sounding between the surface and 1000 m took approximately 20 min, and two soundings per hour were made during most daylight hours. On six occasions this same sounding routine was carried out through the night. The general characteristics of the tethered balloon system are described by *Emmitt* [1978] and *Wylie and Ropelewski* [1980].

Rawinsonde measurements were made at Ducke Reserve at 3-hour intervals during all operations. When operations were confined to daylight hours, soundings were made between 0800 and 1700 (60°W) local standard time (LST). The Ducke soundings were made to an average height of 450 mbar, using a high-resolution Atmospheric Instrumentation Research (AIR) sonde and a digital recording and processing system providing measurements every 25 m.

The NASA Electra aircraft made meteorological and chemical measurements along the flight track and in spirals between 150 m and 5 km above the surface. An airborne ultraviolet differential absorption lidar (UV DIAL), described by *Browell et al.* [this issue], provided measurements of aerosol and ozone concentrations in the vertical column below the aircraft. Extended horizontal flights covering hundreds of kilometers [*Harriss et al.*, this issue] and up to 6 hours of flying time covered a significant fraction of the Amazon basin.

3. ANALYSES

This section presents the techniques used to examine features of the mixed layer and provides a general description of the diurnal characteristics of the mixed layer for undisturbed conditions in terms of composited data. A simple box model is applied to estimate the entrainment fluxes of heat and moisture above the mixed layer during daytime convection. This is followed by application of the "jump" mixed layer model as a technique for estimating the same fluxes without the necessity of measuring the mixed layer height.

A conceptual model of mixed layer growth is useful for the discussion which follows. Three stages of boundary layer growth on undisturbed days are [*Tennekes*, 1973; *Caughey*, 1982] as follows:

1. Surface heating causes erosion of a strong inversion that develops overnight. At this time there is relatively little coupling with the environment above the convectively mixed layer. Since this layer is relatively shallow, we expect changes in surface fluxes to result in relatively large changes in concentration at this stage.

2. There is a rapid rise of the convectively mixed layer, with attendant entrainment flux of air from above becoming important.

3. This is followed by gradual decay of dry convective mixing as the surface buoyancy flux changes sign [*Nieuwstadt and Brost*, 1986].

According to this idealization, a mixed layer only grows upward, entraining and energizing a relatively quiescent fluid. When the layer becomes decoupled from the surface, there is no reason for the layer, originally mixed by buoyant elements rising from the surface, to form strong gradients of nonreact-

ing species. In this circumstance we expect to discover fossil mixed layers that are mixed but no longer mixing.

3.1. *Mixed Layer Heights*

The vertical potential temperature Θ_v is used here for defining the region of convectively driven mixing in which the actively mixing layer will show a neutral profile in Θ_v. This layer is generally capped by a thin, transitional inversion layer. This inversion gives way to a slightly stable atmosphere above. For this paper the bottom of the inversion is used to define the mixed layer depth. This definition is applied during the period of significant heating, i.e., 0700–1700 LST.

The tethered balloon system has a maximum measurement altitude of approximately 1100 m above ground level. On many days the mixed layer would grow above the top of the tethered balloon profile. Thus there are cases when tethered balloon profiles represent measurements made totally within the mixed layer. However, the rawinsonde, aircraft, and lidar measurements were able to track the higher mixed layer, although at less frequent intervals.

Tethered balloon soundings were made on the average of twice an hour. Rawinsonde soundings are available generally at 0800, 1100, 1400, and 1700 LST. In determining a time sequence of mixed layer heights, the balloon and rawinsonde values were plotted together. In the cases where the mixed layer grew above the balloon, heights were interpolated between the rawinsonde soundings. In rare cases the 1700 LST rawinsonde sounding did not show a clear inflection point in Θ_v. This is indicative of the fact that the surface heat flux has been negligible or negative for some time, the mixing layer has stopped warming, and the nocturnal inversion has begun to form and decouple the layer from the surface. In these cases the mixed layer height, as determined by the 1400 LST rawinsonde sounding, was used to specify a constant depth for the remaining part of the afternoon. The interpolated mixed layer heights were used to provide a necessary scaling height in the composite analysis which follows.

For the nocturnal periods, defined here as 1700–0700 LST, the depth of the nocturnal stable layer was also identified as the point where the gradient in Θ_v undergoes a rapid change. In addition, specific humidity q was frequently, although not always, well mixed within the stable layer. Calculations of the bulk Richardson number showed it often to be near-critical, suggesting that mechanical mixing could be maintained in the stable layer in the presence of strong stability.

Tethered balloon and rawinsonde profiles for July 31 are presented in Figure 2, as an example of typical soundings and the mixed layer height determinations. This sequence clearly illustrates the evolution of the daytime mixing layer. As shown by the early morning soundings, the stable nocturnal boundary layer is well established before sunrise. The lapse rate of Θ_v near the surface is approximately 27 K km^{-1} at 0638 LST. In the 0722 and 0753 LST soundings we see the stable layer being eroded by the surface heating, and by 0836 LST the mixing layer has grown to 480 m. In a given profile, as seen at 0836 LST, there often appears a fine structure which shows evidence of thin, intermittant stable layers. In general, one can discern within the time series the mixing layer, which is approximately well mixed and which is capped by an inversion which continues into the unmixed layer above.

The mixing layer grows rapidly and by 1045 LST is near or above 1140 m. The rawinsonde sounding at 1112 shows the height to be 1390 m, which increases to 1530 m at 1410 LST and then increases slowly to 1620 m by 1722 LST. Slow or no growth was commonly observed after the 1400 LST rawinsonde sounding.

The nocturnal stable layer is seen to have begun developing in the 1722 LST sounding, although there is a 100-m shallow mixed layer below the inversion. By 1900 LST the stable layer is clearly established.

3.2. *Disturbed and Undisturbed Days*

A primary goal of this paper is to present a generalized picture of daily mixed layer growth in the Amazon region, along with estimated fluxes. On days with significant convective activity and the associated rain showers, outflows, and cloudiness, the mixed layer will be modified in a random fashion throughout the day. This study has therefore chosen a subset of days from the ABLE 2A experiment which were determined to have minimal convective modification of the mixed layer. A day was classified as representing disturbed conditions if it satisfied one or more of the following conditions:

1. Rainfall equal or greater than 1 mm was reported at any station.
2. One or more periods existed where the surface heat flux and temperature were greatly diminished for longer than an hour.
3. Vigorous cumulus activity was reported for periods longer than an hour.
4. Incoming solar radiation diminished for substantial periods of time, indicating significant cloud cover.

Using these criteria and chosing days for which tethered balloon, rawinsonde, surface flux, and automatic weather station data are available, we are able to identify 7 days which constitute a data set for undisturbed conditions. These days are July 23, 25, 26, 29, 31, and August 2 and 3.

The suite of measurements allows for a detailed description of the mixed layer and the surface conditions associated with it, and made the identification of the undisturbed days straightforward. To illustrate this identification process, Figures 3 and 4 present the combined measurements for a typical disturbed (July 27) and undisturbed day (July 31). On July 27 (Figure 3) the factors identifying it is a disturbed day are evident, with significant rainfall in the afternoon, a sharp decrease in surface heat flux and temperature at 1300 LST, and an early decrease of the incoming solar radiation. We clearly identify the outflow event in the contoured field of Θ_v, which shows a layer of cooler air that reaches from the surface to 800 m.

The disturbed day is clearly contrasted with the undisturbed conditions of July 31 (Figure 4). On this day no rainfall was reported, and surface temperature and solar radiation values show a smooth diurnal progression. Surface fluxes are much smoother than for the disturbed day, and they diminish evenly near the end of the afternoon. The mixed layer grows above the tethered balloon profiles, and this neutrally stable region exists until 1600 LST. The nocturnal stable layer develops quickly after this time.

3.3. *Composite Analysis*

The determination of a general undisturbed condition is presented in this section. The various measurements are averaged with techniques appropriate to the type of measurement.

Surface fluxes and the surface values of temperature T, spe-

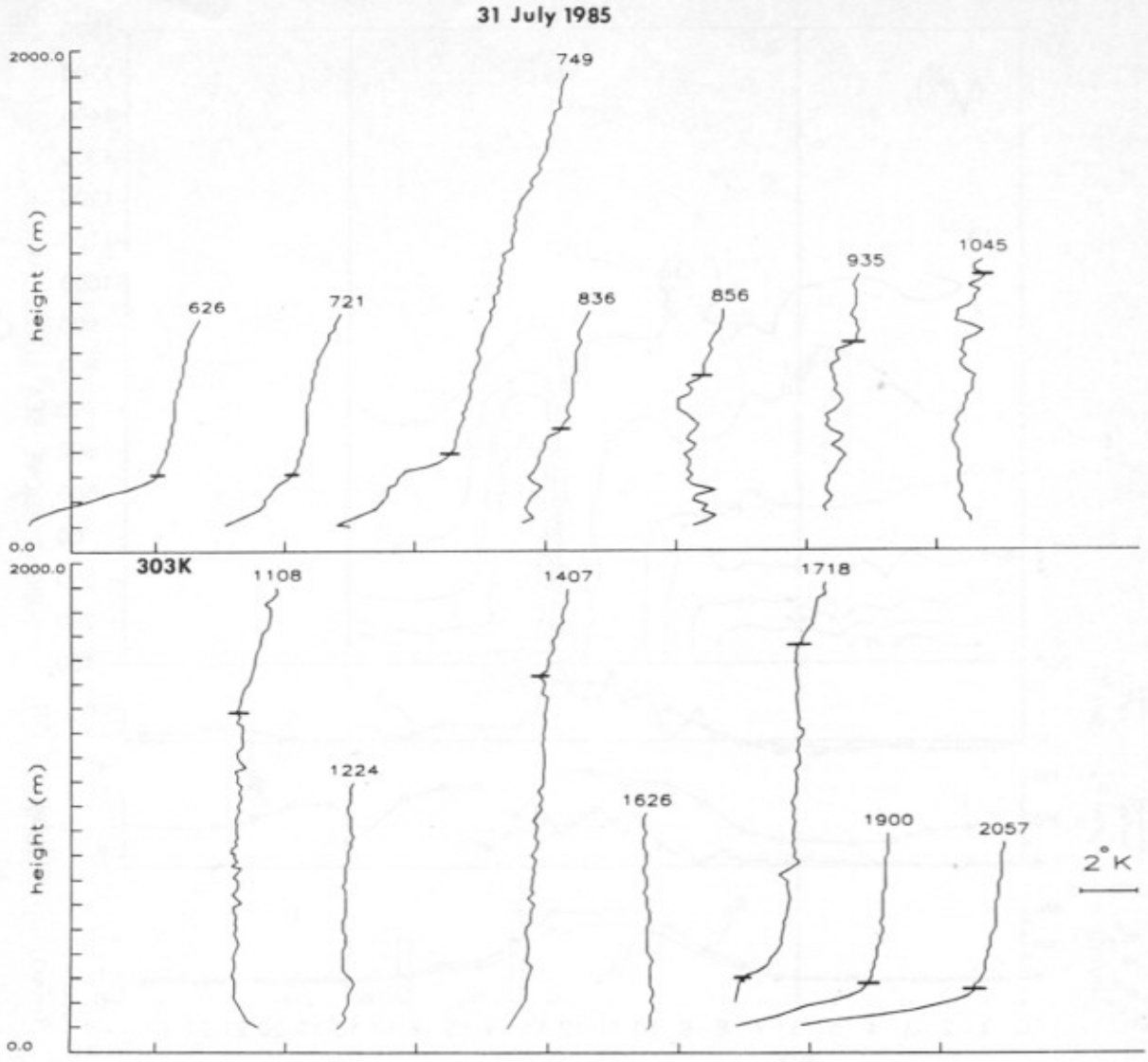

Fig. 2. Tethered balloon and rawisonde profiles of Θ_v made on July 31, 1985. Mixing layer heights are shown by the horizontal line. A reference tick of 303 K is plotted for each profile, and the time (LST) is noted above each profile.

cific humidity q, solar radiation R_s, and net radiation R_n were averaged over hourly intervals. This had the desired effect of smoothing the flux measurements, which exhibit some fairly high frequency variations. T, q, R_s, and R_n are presented as hourly means on a given day. Mixing layer heights were averaged over 2-hour periods, or over 1-hour periods when there was a significant number of profiles for the given hour.

The "jump" mixing layer model, described later, calculates mean values for the mixed layer and uses gradients above the mixed layer as the boundary and initial conditions. For this reason, and because we are interested in documenting the structure of the Amazon mixed layer, a scaling procedure was applied to the tethered balloon profiles. Each profile was scaled by the mixed layer height and divided into an equal number of scaled intervals within the mixed layer. An average per time of day was made at each of these intervals up to the mixed layer height. Above the mixed layer, averages were computed on fixed 20-m intervals. An average profile was reconstructed by assigning the mixed layer averages to equally spaced heights within the mean mixed layer depth and assigning the averages above the mixed layer to 20-m intervals above the mean mixed layer height.

The resulting composite analysis is shown in Figure 5. The rapid growth of the mixed layer is well demonstrated in both the contoured Θ_v field as well as the average mixed layer height. Rapid growth is seen to begin with a mixed layer of 340 m at 0730 LST and to continue to a height of 1050 m at 1130 LST, giving a growth rate of 4.9 cm s^{-1}. Growth continues much more slowly after this time, gaining another 150 m by 1700 LST.

One pronounced feature of the composite analysis, often seen clearly on the disturbed days as well, is a midmorning maximum in q, as measured at the top of the forest canopy, followed by drying throughout the rest of the day (Figure 5). This drying starts at approximately 1030 and continues until nocturnal cooling reestablishes a shallow mixed layer at near 1700. Concurrently, however, there are significant (approximately 400 W m^{-2}) positive fluxes of water vapor across the top of the forest canopy. Entrainment fluxes across the top of the mixed layer must therefore be large for drying to occur in

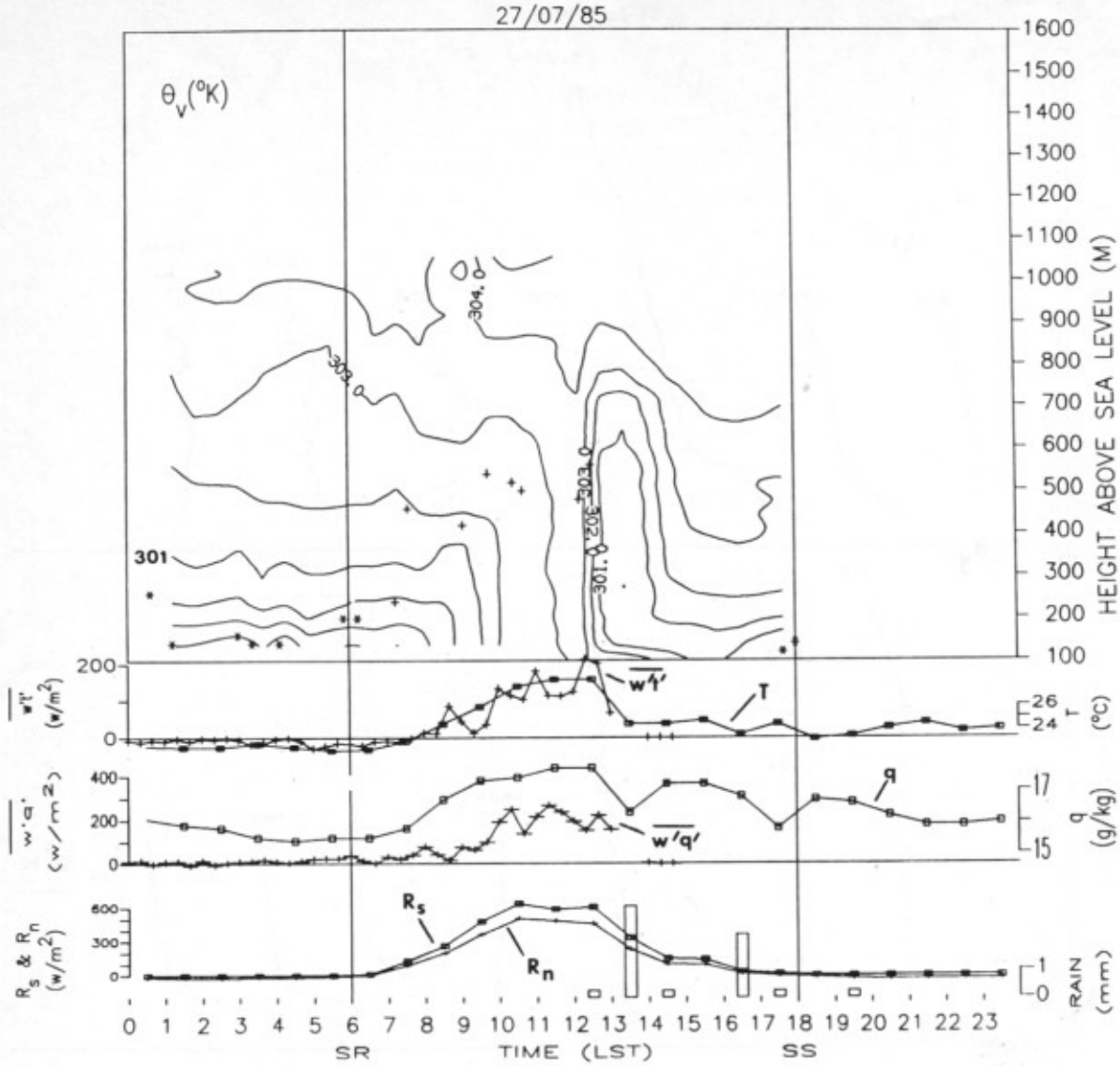

Fig. 3. Data from July 27 (disturbed day). The upper plot shows contours of virtual potential temperature, Θ_v, as measured by the tethered balloon. Observed mixed layer heights are marked with a plus for the tethered balloon and a box for the rawinsonde sounding. The nocturnal stable layer top is marked with an asterisk. The lower three graphs show time series of the heat flux $\overline{w't'}$, temperature T, moisture flux $\overline{w'q'}$, specific humidity q, incoming solar radiation flux R_s, net radiation flux R_n, and rainfall, all measured at the micrometeorological tower. The $\overline{w't'}$ and $\overline{w'q'}$ were measured at the 40-m level; the other parameters were measured at the 45-m level. Hourly totals of rainfall, if present, are designated by a vertical bar. SR and SS are approximate sunrise and sunset.

the mixed layer over the time period 1000–1630 LST, as measured at the top of the canopy. While similar drying by entrainment has been observed close to the tropical ocean during transient periods [*Fitzjarrald and Garstang*, 1981], it appears to be a normal occurrence over the "dry season" rain forest.

The average lifting condensation level (LCL) within the mixed layer was calculated for the 0800, 1100, 1400 and 1700 LST rawinsonde soundings, and these are plotted in Figure 5. The LCL heights follow the mean mixed layer heights, in general being 100 m above the mean mixing layer height. The exception to this is the 1400 sounding, which shows a mean LCL within the mixed layer to be 300 m above the mean mixing layer height, as a result of the afternoon drying noted previously.

Fitzjarrald et al. [this issue] remarked on the frequent periods with small, positive or even negative, sensible heat fluxes observed during the daytime over the Amazon forest. We have seen here that even with such periods, which were observed on the undisturbed days, the convective boundary layer tends to grow above 1000 m, well above the 500-m thickness typically seen over tropical oceans. The net effect of these periods of transient stability on estimates of average transport over large areas is not easy to determine. However, we hypothesize that one consequence is that there must be modulation of the mixing intensity of turbulence in the convective boundary layer, as estimated by the characteristic mixing velocity w^* and mixing time h/w^*. This modulation may be important in interpreting the budget of chemical species whose reaction time is comparable to the turbulent

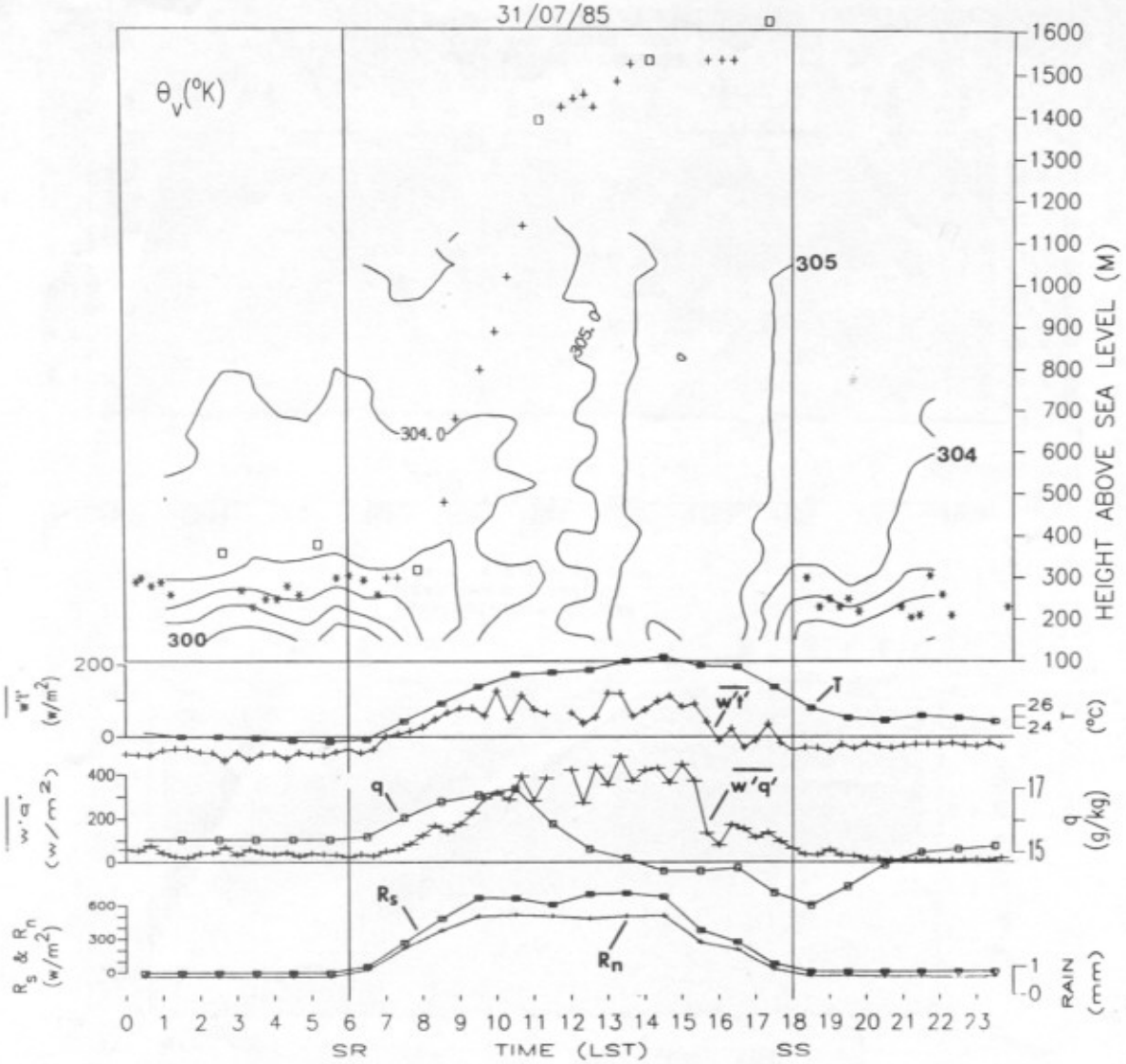

Fig. 4. As in Figure 3, but for July 31 (undisturbed day).

mixing time. This effect has been noted for atmospheric turbulence in the surface layer [*Lenschow et al.*, 1982; *Fitzjarrald and Lenschow*, 1983] for the ozone–nitrogen oxide smog reaction and may be important in the boundary layer for other species. Characteristic mixing times, together with extreme daytime values, are shown in Table 2.

The mean thickness of the nocturnal stable layer, as shown in Figure 5, is of the order of 250 cm. This is comparable to other observations; e.g., *Nieuwstadt* [1984] reports for Cabauw, Holland, a layer ranging between 70 and 420 m in depth, with a mean thickness of 190 m.

3.4. *Large-Scale Measurements*

The frequency and vertical height resolution of the tethered balloon and rawinsonde measurements provide the best local measurement of the depth of the mixed layer. We now present evidence that the observations made at a single point (Ducke Reserve) may be representative of a much larger area.

Figure 6*a* shows mixed layer heights, as determined from the aircraft spiral soundings taken over many different locations [*Harriss et al.*, this issue], as a function of time of day. The growth pattern on undisturbed days (Figure 6*b*) is very similar to the mean mixed layer heights determined by the tethered balloon and rawinsonde measurements (Figure 5) at a fixed point.

Heights obtained from UV DIAL versus aircraft spiral soundings for undisturbed conditions are shown in Figure 7. Except for a slight tendency (less than 100 m on average) to overestimate the mixed layer height from the lidar, the agreement is excellent (correlation coefficient of 0.96). We conclude from the preceding that the special radiosonde and the aircraft in situ and remote (UV DIAL) methods represent viable tools for examining the behavior of the mixed layer over longer time scales and greater distances.

Plate 1 shows lidar observations on an undisturbed day (August 21) which cover a large region (see Figure 1 for flight track) of the tropical rain forest. Measurements begin at 0916 LST (1316 UT) and continue to 1223 LST (1623 UT) thus covering the time of maximum mixed layer growth. Plate 1 (top panel) starting at 0916 LST, shows a mixed layer is evi-

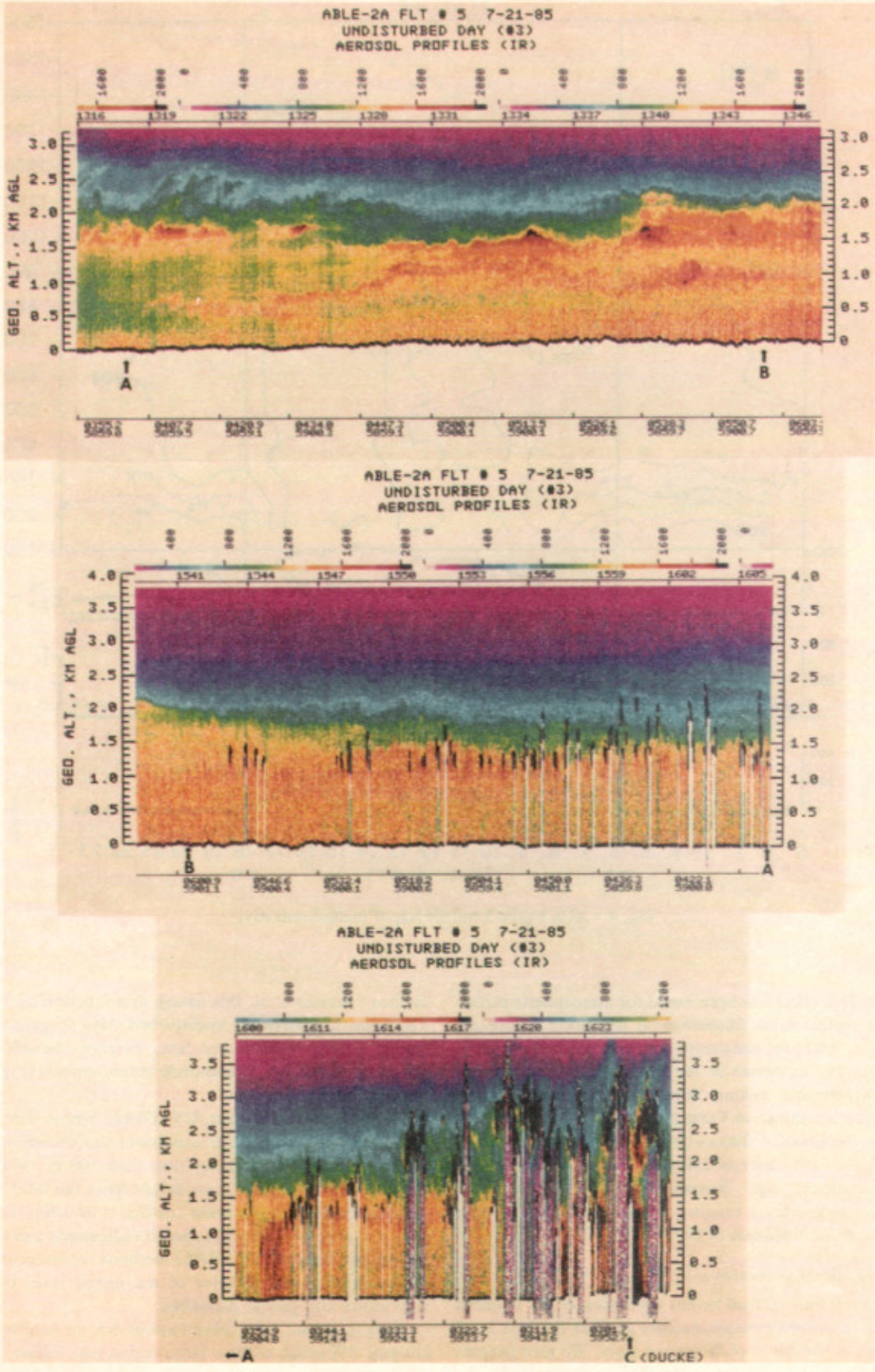

Plate 1. UV DIAL measurements made during undisturbed conditions on July 21. Universal time appears above the color trace. The color bars above the time provide a key to UV DIAL values. Latitude and longitude are shown below the color trace. (Top) 1316–1346 UT. (Middle) 1541–1605 UT. (Bottom) 1600–1623 UT.

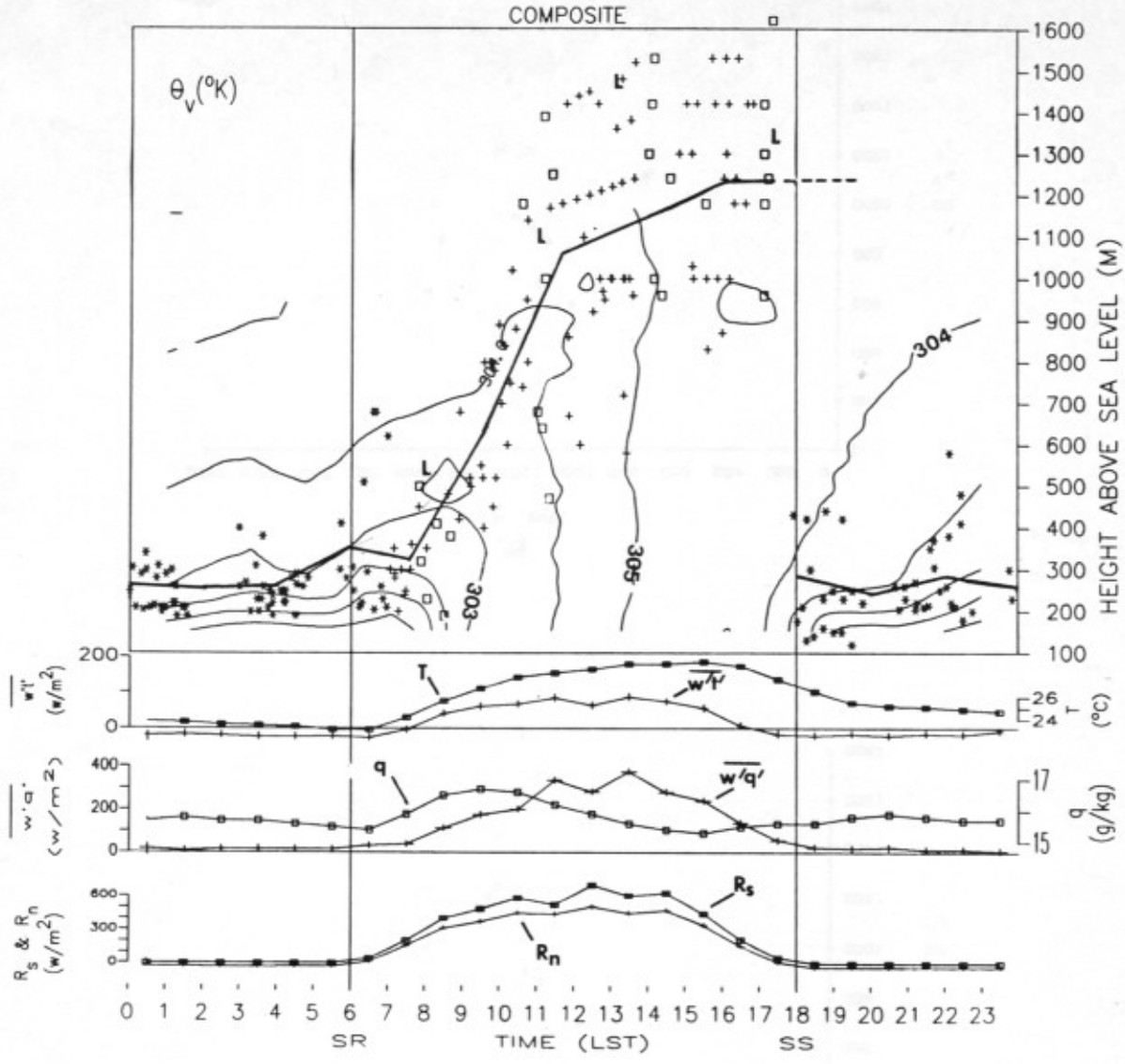

Fig. 5. As in Figure 3, for the composited data set consisting of days July 23, 25, 26, 29, 31, and August 2 and 3. In addition, the mean mixed layer height (solid line) and mean rawinsonde determined LCL heights within the mixed layer (L) are plotted.

dent to 250 m, near point A, and is growing along the flight track to 500 m near point B at 0946 LST. By the next high level pass (Plate 1, middle panel) starting at 1140 LST, the mixed layer has grown to 1100 m near point B (growth rate of 8.8 cm s^{-1}), after which it slowly rises to about 1200 m at 1206 near point A (growth rate of 9.3 cm s^{-1}). The mixed layer has about the same depth until convective activity increases during the final leg near Ducke (Plate 1, bottom panel). Successive lidar measurements under undisturbed conditions show the same behavior of the mixed layer. There is no evidence that over the vast regions of rain forest around Manaus, the growth rate of the mixed layer shows any major spatial variations due to subtle changes in the underlying surface. The very rapid growth of the mixed layer exhibited in the early growth phase, as observed by lidar, agrees with the growth rates based upon in situ measurements.

3.5. *Entrainment Flux Estimates*

A simple box calculation is next employed to estimate the entrainment fluxes of moisture across the top of the mixed layer. The following budget equation is utilized:

$$dq_m/dt = (F_{q,0} - F_{q,h})/h \tag{1}$$

where q_m is the mixed layer mean value of q, $F_{q,0}$ is the surface flux of q, $F_{q,h}$ is the entrainment flux of the q at the top of the mixed layer, and h is the depth of the mixed layer. The observed values of q, h, and the surface moisture flux are used

TABLE 2. Characteristic Mixing Times

Date	Time, LST	h, m	$\overline{w'\theta_v'}$, w m^{-2}	w^*, m s^{-1}	t, min
July 25	0951	650	100	1.19	9.1
July 25	1215	840	100	1.30	10.7
July 25	1325	440	180	1.27	5.8
July 31	0856	430	60	0.88	8.1
July 31	1045	1090	120	1.50	12.1

Here $t = h/w^*$, where w^* is the mixing velocity and h is the mixed layer depth. The reference temperature θ_{v0} is taken to be 300°K, and w^* is given by $w^* = (g\overline{w'\theta_v'}h/\theta_{v0})^{1/3}$.

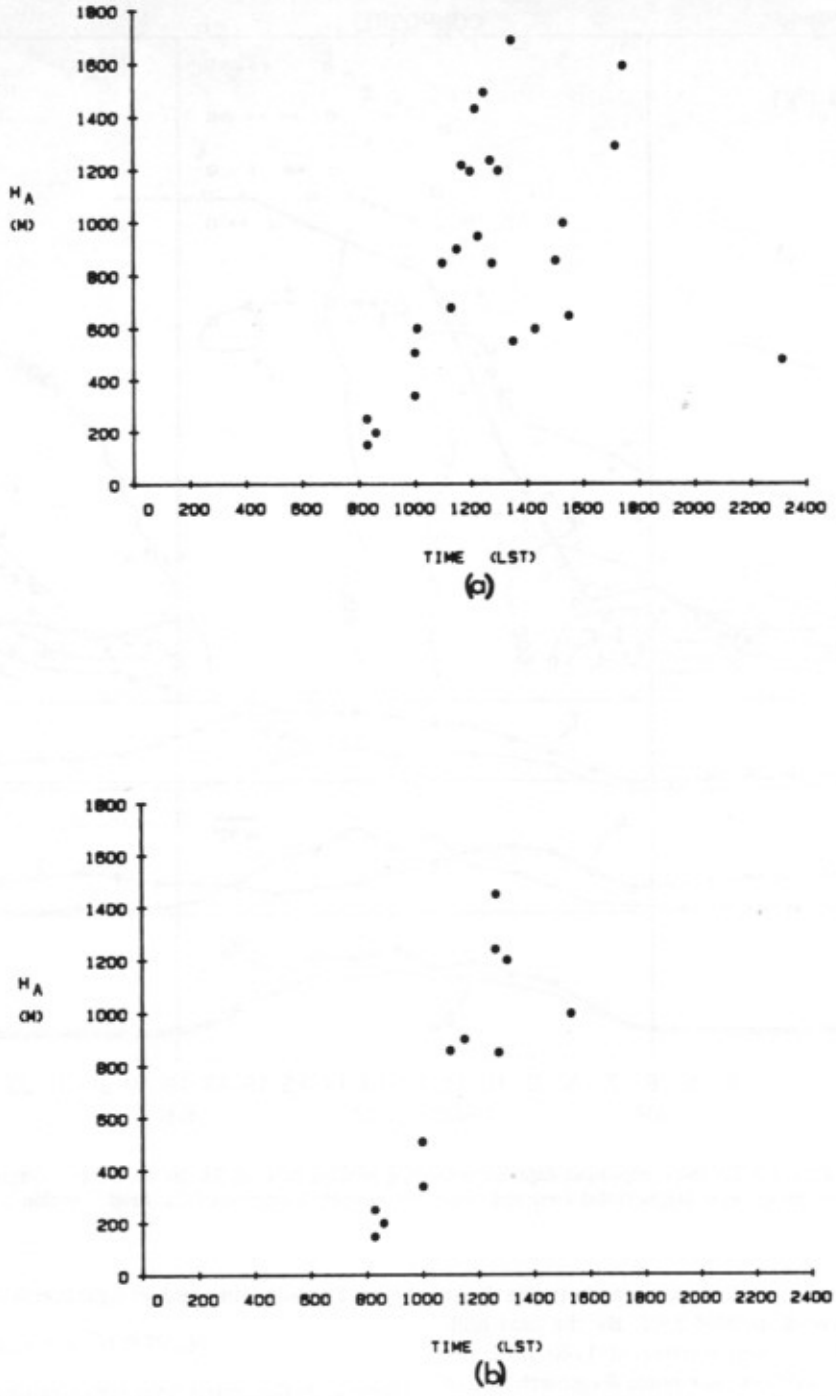

Fig. 6. Mixed layer height, as determined by the aircraft (H_A). (*a*) All days. (*b*) Undisturbed days.

with (1) to make the direct estimate of the entrainment moisture flux. In this case, q measured at the micrometeorological tower was taken to represent average value in the mixing layer. This budget calculation was done for the composited data set in order to estimate the mean value of the entrainment moisture flux over time for the mixing layer. We assume that advective influences will be negligible in the composite data set, and therefore advective terms are not included in (1).

The results shown in Figure 8 clearly demonstrate that the entrainment moisture flux across the top of the mixed layer must approach 600 W m^{-2} to produce realistic mixed layer drying rates. The significance of this finding is enhanced by the fact that the observed entrainment depends primarily upon knowledge of the mixed layer depth. Two points can be made here: (1) if the difference in concentration between the mixed layer and the environment above is large enough, entrainment fluxes will dominate concentrations in the mixed layer even in the presence of very large surface fluxes, and (2) estimated fluxes into the deeper atmosphere will depend not only on the measured surface flux and concentration of a quantity, but upon mixed layer depth and rate of growth.

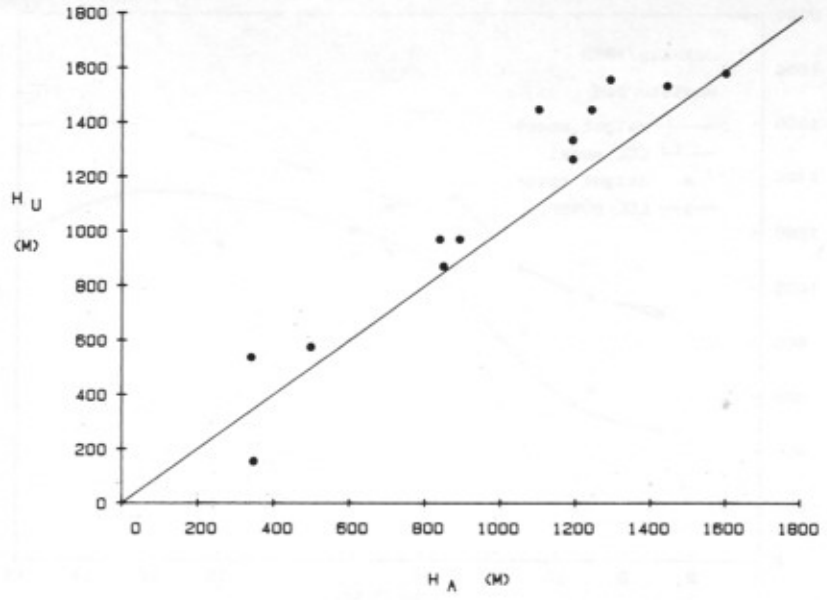

Fig. 7. Comparison of aircraft (H_A) and UV DIAL (H_U) determinations of mixed layer height.

3.6. *Application of the "Jump" Model*

The simple "jump" model of mixed layer growth [*Tennekes*, 1973; *Betts*, 1973] is utilized next to estimate entrainment fluxes. The model is forced by observed surface fluxes and is bounded by the initial mixed layer mean and the gradients above the mixed layer.

This model assumes zero gradients of Θ_v, q, and concentrations of trace substances in a mixed layer, with a finite jump in each quantity at the mixed layer top. The mixed layer mean for any of these quantities, X_m, where X is Θ_v, q, or another species concentration, is:

$$dX_m/dt = (F_{X,0} - F_{X,h})/h \tag{2}$$

where h is the mixed layer thickness, $F_{X,0}$ is the surface flux of a quantity and $F_{X,h}$ is the entrainment flux of X out of the mixed layer at the top. $F_{X,0}$ is obtained from measurements. Entrainment at h is related to the "jump" in X at h,

$$F_{X,h} = (X_h - X_m)w_{en} \tag{3}$$

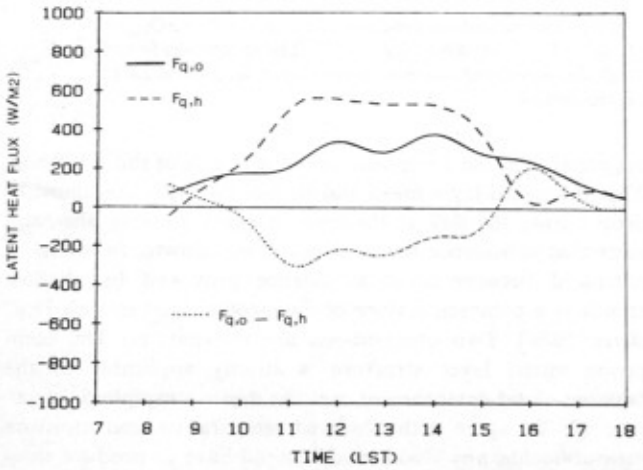

Fig. 8. Entrainment fluxes calculated from a simple budget. $F_{q,0}$, $F_{q,h}$, and $F_{q,0} - F_{q,h}$ are plotted.

where X_h is the value of the quantity above the mixed layer, and w_{en} is the entrainment velocity, given as $dh/dt - w_h$. Environmental subsidence is given by w_h. When the mixed layer grows into a layer exhibiting vertical gradient Γ_X, X_h changes according to

$$dX_h/dt = \Gamma_X w_{en} \tag{4}$$

We apply the standard closure assumption [*Driedonks*, 1982]:

$$F_{\Theta v,h} = -0.20\, F_{\Theta v,0} \tag{5}$$

We assume, as with the simple budget, that local advective effects would not be systematic enough to appear in the mean.

Our aim is to estimate the required mixing layer growth to achieve the observed stratification and the observed surface fluxes. We hypothesize that the entrainment flux of any other constituent during the morning growth phase could similarly by estimated, given surface fluxes of the constituent and buoyancy along with a time series of the mixed layer heights.

Driedonks [1982] presented a series of comparisons of predictions of this model with more complex entrainment parameterizations. He found that the simple model yielded acceptable predictions of mixed layer height and noted that increasing the complexity of the entrainment parameterization did not noticeably improve the prediction.

Because morning tethered balloon profiles did not always go beyond 600 m, we used gradients for Θ_v and q above the mixed layer obtained from an average of five early-morning radiosonde ascents on undisturbed days. Taking the initial conditions to be the composite mixed layer mean values of q and Θ_v at 0830 LST (the first averaging period for which the nocturnal surface inversion filled in), and using the observed composite surface buoyancy flux, we simulated mixed layer growth with the simple model. The model results were compared with composite data and showed good agreement until about noon, after which the model predicted mixed layer heights that were too large. At this point, observed and modeled mixed layer heights approached 80% of the value of the lifting condensation level, and it is plausible that shallow

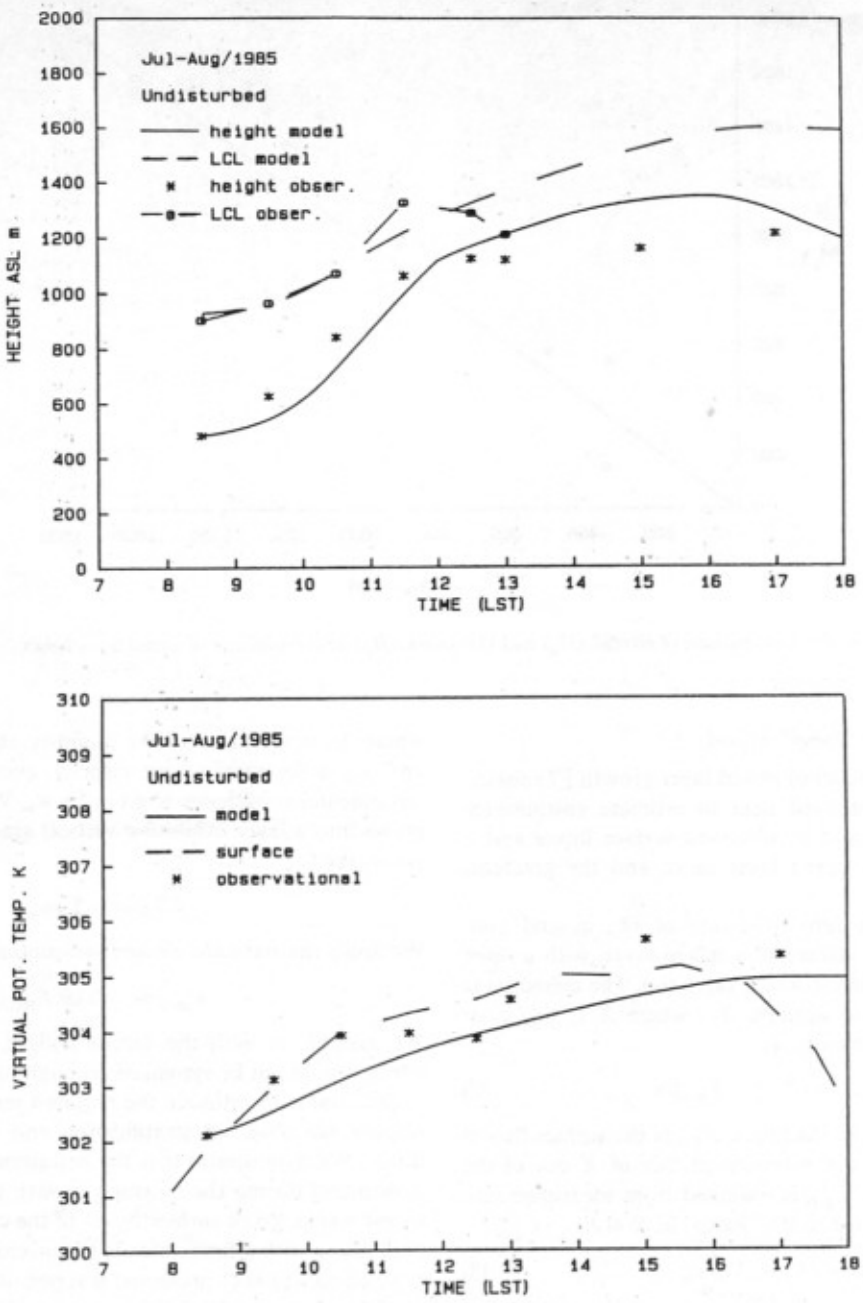

Fig. 9. Comparison of model results with composite data. Initial and boundary conditions are $h = 430$ m, $\Theta_{v,m} = 302.1$ K, $\Theta_{v,h} = 302.9$ K, $q_m = 14.8$, $q_h = 13.6$ g/kg, $\Gamma_{\Theta_v} = 0.0019$ K m^{-1}, $\Gamma_q = -0.0040$ g kg^{-1} m^{-1}. The model was forced with the composited moisture and buoyancy fluxes (Figure 5). (Top) Simulated and observed mixed layer height and *LCL*; (bottom) simulated and observed mixed layer mean $\Theta_{v,m}$ and θ_v at the surface.

clouds could have led to enhanced subsidence. We included afternoon between cloud subsidence here by imposing a constant mean subsidence of -0.028 m s^{-1} on model growth after noon. This value was selected to give rough agreement with observations of mixed layer height and temperature, with the results shown in Figure 9. The subsidence is similar to values of -0.017 m s^{-1} diagnosed using the mixed layer model by *Fitzjarrald* [1982] for undisturbed mixed layers in conditions of shallow convection over the tropical ocean during GATE and of -0.021 m s^{-1} found by *Oliveira* [1985] for undisturbed days over land in the state of São Paulo, Brazil.

Observed stability above the mixed layer did not change appreciably in the composite over the course of the afternoon. That the mixed layer mean and surface humidity continued to drop during the day as the layer stopped growing also suggests that subsidence limits mixing layer growth. In addition, enhanced between-cloud subsidence provoked by shallow clouds is a common feature of diagnostic cloud models [e.g., *Betts*, 1976]. Two observations are relevant: (1) The composite mixed layer structure is strictly applicable to the between-cloud environment, not the mean atmospheric structure. (2) To agree with observed temperature and moisture measurements, any cloud model would have to produce similar subsidence estimates.

The model allows us to estimate the moisture flux $F_{q,h}$ at

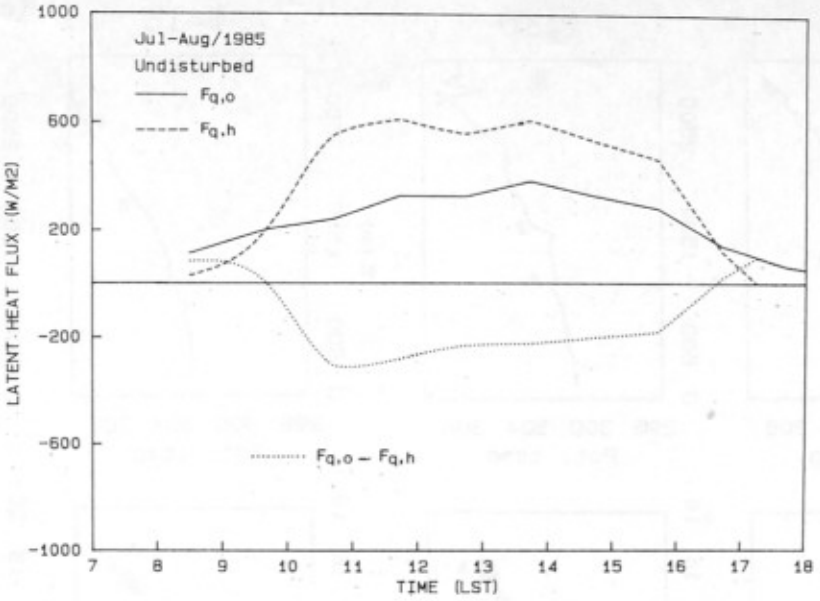

Fig. 10. Time series from model results of moisture flux at the surface ($F_{q,0}$), the entrainment flux ($F_{q,h}$), and the difference $(F_{q,0}) - (F_{q,h})$.

the mixed layer top, as shown in Figure 10. The estimated values agree remarkably well with the earlier budget calculations (Figure 8). Thus by allowing for an appropriate subsidence and using appropriate initial and boundary conditions along with the observed surface fluxes, the model is able to simulate a realistic mixing layer budget of a species.

3.7. *Mixing Line Analysis*

Clouds mix moisture emitted from the surface through a deeper layer. Conservative variable analysis can give some clues as to the depth of the moist convective mixing [*Betts*, 1985]. The analysis states that simple mixing of air having characteristic values at condensation level results in conservative properties that are linear fractions of the endpoint conditions, giving rise to an identifiable "mixing line."

Figure 11 presents a plot of equivalent potential temperature Θ_e at saturation point (here the lifting condensation level) versus its specific humidity, for 23 undisturbed rawinsonde soundings made between 1000 and 2200 LST. It shows that, broadly speaking, a mixing line relationship exists from the surface to 3 km (approximately 710 mbar). However, we must draw a clear distinction between mixing and mixed layers over land. There is active coupling below 3 km only during the daytime, but the results of the mixing persist through the night in the form of fossil mixed layers. These layers start the evening well mixed in moisture and potential temperature and persist on occasion to the following morning. Inferring transports based on mixing line structure, as has been done for the oceanic trades [*Betts and Albrecht*, 1987] will only be meaningful over the Amazon during the day.

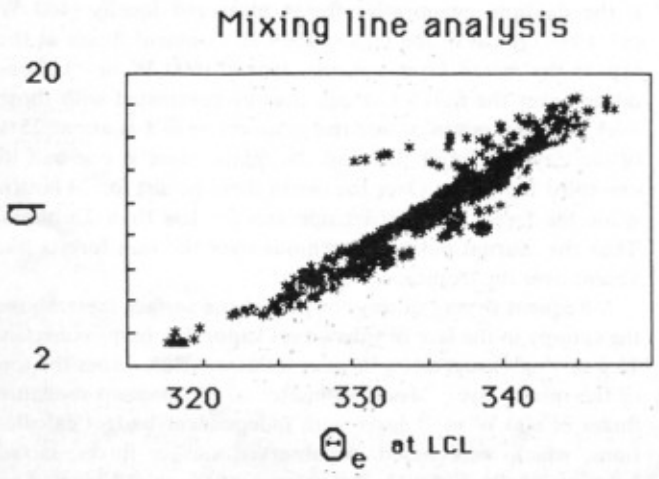

Fig. 11. Mixing line analysis for 23 soundings made between 1000 and 2200 LT.

We can illustrate a typical mixing sequence with a series of four soundings to 3000 m made on a typical undisturbed day (July 21, Figure 12). Here Θ is plotted on the upper diagram. In the lower plot is the mixing line diagram, which shows q at the LCL as a function of Θ_e. Note that points which are widely separated in height on the Θ diagram can be coincident on the mixing line diagram.

Three distinct layers are evident in the 0847 LST sounding: (1) The growing new dry convectively mixed layer (labeled A in the Θ profile and on the mixing line diagram); (2) a layer extending up to B in the Θ profile, which we take to be the remnants of the previous day's convective boundary layer, mixed but not mixing; and (3) a cloud layer. The large cluster of points at B on the mixing line diagram identify the homogeneous "fossil" mixed layer.

By the 1100 LST sounding the mixing layer has destroyed the nocturnal stable inversion and is growing rapidly in the environment of the previous day's mixed layer. The point cluster at A on the mixing line shows the well-mixed region which extends from the surface to A in the Θ diagram. Between A and B is a gradient in q and Θ_e, as the mixed layer blends with the fossil layer. The remnants of the fossil layer are still evident in the group of points at B on the mixing line. Reported conditions were approximately saturated at level C at 1110, probably due to the sonde penetrating cloud.

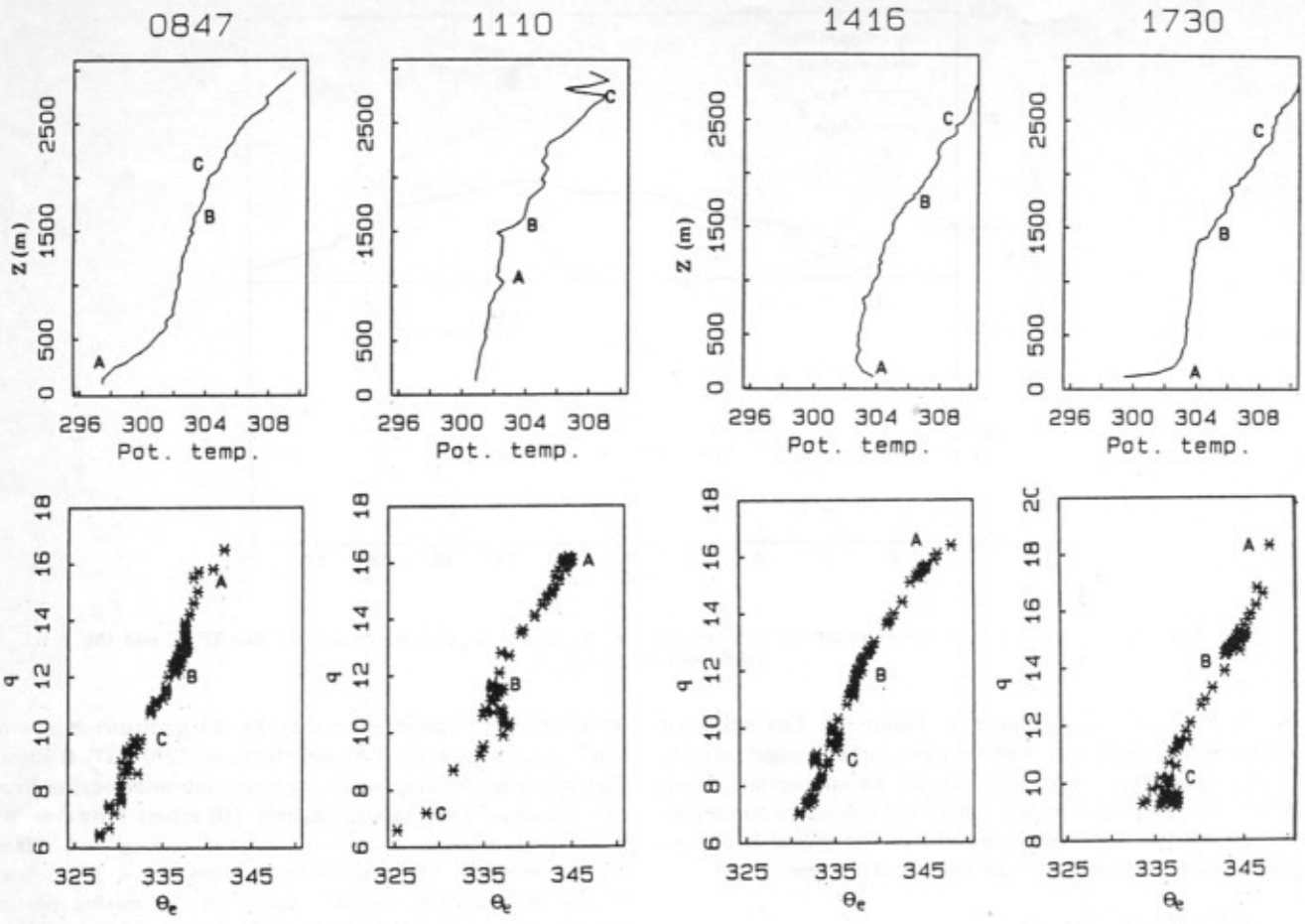

Fig. 12. Sequence of potential temperature profiles and mixing line diagrams made from soundings on July 21, 1985. Points marked with letters on the profiles correspond to those indicated on mixing diagrams.

By 1416 LST, dry convective mixing extended to approximately 1500 m. Note that there was an appreciable moisture gradient within the convective boundary layer (from A to B, along a mixing line) and that the cloud layer data appears to lie on a different mixing line. At 1730 the stable boundary layer reappeared (A), the fossil mixed layer was present up to level B, and the cloud layer (C) was left decoupled from the surface.

4. Discussion

The observations of ABLE 2A provide an initial description of the structure and growth of the atmospheric mixed layer over an equatorial rain forest during the "dry" season. A coherent picture emerges when emphasis is placed upon those days showing undisturbed conditions.

Radiative cooling of the forest canopy results in a marked surface inversion, with stratified conditions developing rapidly, even before sunset. Sensible heat fluxes are usually negative an hour before sunset and remain negative throughout the night. Mixed layer growth begins soon after sunrise as the surface sensible heat flux becomes positive. Maximum rates of growth of up to 10 cm s^{-1} can be reached within 2 hours of sunrise. The mixed layer under undisturbed conditions typically reaches 1000 m by 1100 LST, remaining above this altitude until 1600 LST. Thus mean mixed layer growth rates are of the order of 5 cm s^{-1}. Maximum depth of the mean mixed layer is reached by 1300 LST and is observed to reach a height of 1200 m.

No horizontal discontinuities were noted in the mixed layer depth over distances of 300–400 km under undisturbed conditions. Growth rates and the general behavior of the mixed layer, as determined locally, were duplicated over a very large region of rain forest around Manaus. This would suggest that if the daytime evaporative fluxes measured locally (400 W m^{-2}) are typical of the region, then entrainment fluxes at the top of the mixed layer are also typical (600 W m^{-2}). Conditions over the rain forest can thus be contrasted with those over the open ocean, where the evaporative flux is about 25% of the daytime forest flux and the mixed layer is one-half to one-third the depth. Over the ocean these persist for 24 hours, while the forest counterpart operates for less than 12 hours. Thus the diurnal pulse is enormous over the rain forests but absent over the tropical oceans.

A frequent drying during the day in the surface layer above the canopy in the face of substantial vapor flux (approximately 16 g m^{-2} s^{-1}) suggests a large entrainment flux across the top of the mixed layer. Model estimates of entrainment moisture fluxes of 600 W m^{-2} agree with independent budget calculations, which were based on observed surface fluxes, mixed layer specific humidity, and the depth of the mixed layer. Any estimate of the mixed layer budget of a trace chemical must, by these findings, take the entrainment flux into consideration.

These results apply to the between-cloud environment and represent mean atmospheric conditions. To arrive at acceptable model estimates, however, cloud-induced subsidence had to be assumed. Characteristic turbulent mixing times for the growing mixing layer were found to be of the order of 10 min.

Vertical profiles of the saturation point, as represented by the lifting condensation level, show a typical sequence as the new dry convective layer replaces the previous day's convective boundary layer and builds into the cloud layer. The active coupling exists only during the daytime and will represent the only time during which vertical transports can be inferred from the mixing line structure.

We conclude that if the difference between the concentrations in the mixed layer and above the mixed layer is large enough, entrainment fluxes across the top of the mixed layer will dominate the balance in the mixed layer, even in the presence of large surface layer fluxes. This conclusion implies that any estimate of the fluxes across the top of the mixed layer will depend upon knowledge of the growth and depth of the mixed layer. It was shown that in a composite sense the "jump" mixed layer model is a reasonable substitute for actual mixed layer measurements.

Fluxes of water vapor across the canopy under undisturbed conditions appear to be relatively well behaved. The UV DIAL aerosol measurements supply estimates of the depth of the mixed layer. Concurrent measurement of the water vapor profile would provide an estimate of the vapor flux across the top of the mixed layer. Such measurements could be made over large areas under undisturbed conditions.

The ABLE 2A findings suggest that we can now make some estimates of water vapor fluxes over wide areas of the Amazon basin between clouds and under undisturbed conditions. These estimates can be made with the greatest certainty for those times and places where the aircraft measurements were made. Greater uncertainties would appear if these estimates were applied to the fair-weather regions of the basin as a whole, particularly where the underlying terrain and vegetation differ from the Manaus region. We believe, however, that this would represent a substantial improvement in our current knowledge of boundary layer structure and process over this important region. Extending these findings to encompass the disturbed conditions of the wet season is the next major task.

Acknowledgments. The work presented in this paper was funded by grants awarded by NASA to Simpson Weather Associates, the University of Virginia, and the Atmospheric Sciences Research Center, State University of New York, Albany. Manuscript preparation was performed by Mary Morris and Karen Emmitt. Data processing was provided by Jay Boisseau and Curt Burmeister and drafting and proofing by Debby Martin. Data from the automatic weather station were processed by researchers at the Institute of Hydrology, in the United Kingdom, and provided by G. Fisch at the National Institute for Amazon Studies (INPA), Manaus. A. P. Oliveira acknowledges support from the Fundacão de Amparo a Pesquisa do Estado de São Paulo (FAPESP), Processo 86/1263-6, for graduate studies at the State University of New York, Albany. The authors wish to express their deep appreciation for all of the abovementioned assistance and to each of the participants in ABLE 2A, all of whom contributed to the success of the experiment.

REFERENCES

Betts, A. K., Non-precipitating cumulus convection and its parameterization, *Q. J. R. Meteorol. Soc.*, *99*, 178–196, 1973.

Betts, A. K., The thermodynamic transformation of the tropical subcloud layer by precipitation and downdrafts, *J. Atmos. Sci.*, *33*, 1008–1020, 1976.

Betts, A. K., Mixing line analysis of clouds and cloudy boundary layers, *J. Atmos. Sci.*, *42*, 2751–2763, 1985.

Betts, A. K., and B. A. Albrecht, Conserved variable analysis of the convective boundary layer over the tropical oceans, *J. Atmos. Sci.*, *44*, 83–99, 1987.

Browell, E. V., G. L. Gregory, R. C. Harriss, and V. W. J. H. Kirchhoff, Tropospheric ozone and aerosol distributions across the Amazon basin, *J. Geophys. Res.*, this issue.

Caughey, S. J., Observed characteristics of the atmospheric boundary layer, in *Atmospheric Turbulence and Air Pollution Modelling*, edited by F. T. M. Nieuwstadt and H. van Dop, pp. 107–138, D. Reidel, Hingham, Mass., 1982.

Driedonks, A. G. M., Models and observations of the growth of the boundary layer, *Bound. Layer Meteorol.*, *23*, 283–306, 1982.

Emmitt, G. D., Tropical cumulus interaction with and the modification of the subcloud layer, *J. Atmos. Sci.*, *35*, 1485–1502, 1978.

Fishman, J., P. Minnis, and H. G. Reichle, Jr., Use of satellite data to study tropospheric ozone in the tropics, *J. Geophys. Res.*, *91*, 14,451–14,465, 1986.

Fitzjarrald, D. R., New applications of a simple mixed layer model, *Bound. Layer Meteorol.*, *22*, 431–453, 1982.

Fitzjarrald, D. R., and M. Garstang, Boundary-layer growth over the tropical ocean, *Mon. Weather Rev.*, *109*, 1762–1772, 1981.

Fitzjarrald, D. R., and D. H. Lenschow, Mean concentration and flux profiles for chemically reactive species in the atmospheric surface layer, *Atmos. Environ.*, 17, 2505–2512, 1983.

Fitzjarrald, D. R., B. L. Stormwind, G. Fisch, and O. M. R. Cabral, Turbulent transport observed just above the Amazon forest, *J. Geophys. Res.*, this issue.

Harriss, R. C., et al., The Amazon Boundary Layer Experiment (ABLE 2A): Dry season 1985, *J. Geophys. Res.*, this issue.

Lenschow, D. H., R. Pearson, Jr., and B. B. Stankor, Measurements of ozone vertical flux to ocean and forest, *J. Geophys. Res.*, *87*, 8833–8837, 1982.

Logan, J. A., and V. W. J. H. Kirchoff, Seasonal variations of tropospheric ozone at Natal, Brazil, *J. Geophys. Res.*, *91*, 7875–7882, 1986.

National Academy of Sciences, *Global Tropospheric Chemistry*, 194 pp., National Academy Press, Washington, D. C., 1984.

Nieuwstadt, F. T. M., Turbulent structure of the stable, nocturnal boundary layer, *J. Atmos. Sci.*, *41*, 2202–2216, 1984.

Nieuwstadt, F. T. M., and R. A. Brost, The decay of convective turbulence, *J. Atmos. Sci.*, *43*, 532–546, 1986.

Oliveira, A. P., Evolucao da camada limite planetaria e implicacoes na qualidade do ar. M. S. thesis, Univ. de Sao Paulo, Brazil, 1985.

Shuttleworth, W. J., et al., Eddy correlation measurements of energy partition for Amazonian forest, *Q. J. R. Meteorol. Soc.*, *110*, 1143–1162, 1984.

Tennekes, H., A model for the dynamics of the inversion above a convective boundary layer, *J. Atmos. Sci.*, *30*, 558–567, 1973.

Wylie, D. P., and C. F. Ropelewski, The GATE Boundary Layer Instrumentation System (BLIS), *Bull. Am. Meteorol. Soc.*, *61*, 1002–1011, 1980.

E. Browell, Atmospheric Sciences Division NASA Langley Research Center, Hampton, VA 23665.

D. Fitzjarrald, Atmospheric Sciences Research Center, State University of New York, 100 Fuller Road, Albany, NY 12205.

M. Garstang and S. Greco, Department of Environmental Sciences, Clark Hall, University of Virginia, Charlottesville, VA 22903.

C. L. Martin, Simpson Weather Associates, Incorporated, 809 East Jefferson Street, Charlottesville, VA 22902.

A. P. Oliveira, Departamento de Meteorologia, Instituto Astrônomico e Geofisico, Caixa Postal 30627, Universidade de São Paulo, São Paulo, SP, CEP 01051, Brazil.

(Received March 26, 1987;
revised August 20, 1987;
accepted August 20, 1987.)